ELSEVIER

www.elsevier.nl/locate/jorganchem

Journal of Organometallic Chemistry 584 (1999) 33–43

Journal of Organometallic Chemistry

Mechanistical studies on C–H activation reactions of benzaldimines using selectively deuterated ligands: synthesis and crystal structures of $[\mu_2\text{-}\eta^3\text{-}(R)N-CH_2-\overline{C=C-C(H)=C(H)-C(H)=C}(H)]Fe_2(CO)_6$

Wolfgang Imhof [a,*], Angela Göbel [a], Dietmar Ohlmann [a], Joachim Flemming [b], Hartmut Fritzsche [b]

[a] *Institut für Anorganische und Analytische Chemie der Universität, August-Bebel-Straße 2, D-07743 Jena, Germany*
[b] *Institut für Molekularbiologie der Universität, Winzerlaer Straße 10, D-07745 Jena, Germany*

Received 10 January 1999

Abstract

The reaction of $Fe_2(CO)_9$ with imine ligands derived from benzaldehyde leads to the formation of dinuclear iron cluster compounds of the general formula $[\mu_2\text{-}\eta^3\text{-}N-CH_2-\overline{C=C-C(H)=C(H)-C(H)=C}(H)]Fe_2(CO)_6$ by a C–H activation/1,3-hydrogen shift reaction sequence. Six cluster compounds with alkyl and aryl substituents bound to nitrogen have been synthesised and characterised, five of them also by means of X-ray crystallography. The mechanism of the reaction has been investigated by the use of ligands being selectively deuterated in the 2-position. By several NMR experiments including deuterium spectra it can be demonstrated that the hydrogen/deuterium atom of the activated aromatic C–H bond is transferred to the former imine carbon atom producing a methylene group instead and that this reaction strictly follows an intramolecular pathway. © 1999 Elsevier Science S.A. All rights reserved.

Keywords: C–H activation; Iron; Imines; Deuterium-NMR; X-ray

1. Introduction

The understanding of C–H activation processes is a field of research with growing interest especially with respect to the development of catalytic C–C bond formation reactions. Due to this fact both inter- and intramolecular C–H activation reactions have been intensively studied and thoroughly reviewed in the last years [1]. In recent times C–H activation reactions of aromatic imines or ketones have been used to develop catalytic C–C coupling reactions with CO and/or a wide variety of olefins using $Ru_3(CO)_{12}$ or mononuclear ruthenium complexes as catalysts [2]. To get a deeper insight into these catalytic reactions which include C–H activation steps we are interested in the reactivity of α,β-unsaturated imines towards metal carbonyls of Group 8 metals. It is well known that 1-azadiene ligands react with $Fe_2(CO)_9$ to give mononuclear complexes of the type (η^4-azadiene)$Fe(CO)_3$ [3]. Their reactivity [4] is distinctively different compared with the related (1,3-butadiene)$Fe(CO)_3$ [5] and (1,4-diazadiene)$Fe(CO)_3$ [6] complexes. We recently synthesised a series of (1-azadiene)$Fe(CO)_3$ complexes and characterised them by means of single-crystal X-ray diffraction [7]. In contrast to cinnamaldehyde derivatives, α,β-unsaturated imines in which the C–C double bond is part of a heterocyclic or carbocyclic aromatic system react with $Fe_2(CO)_9$ by means of a C–H activation reaction in β-position to the exocyclic imine group [8]. The reaction then proceeds via a 1,3-hydrogen shift reaction to produce a $\mu_2\text{-}\eta^3$-enyl–amido ligand bridging a $Fe_2(CO)_6$ moiety. The first compounds of this type has first been reported in Ref. [8c,f] where the reactions of benzylideneaniline derivatives with $Fe_2(CO)_9$ have been

* Corresponding author. Tel.: +49-3641-948114/488; fax: +49-3641-948102.
E-mail address: cwi@rz.uni-jena.de (W. Imhof)

PII: S0022-328X(99)00082-0

described. The same cluster compound is also available from the reaction of $Fe_3(CO)_{12}$ with benzalazine [9]. Structural information is only available for the cluster compounds described in Refs. [8f,9b] as well as for a substitution product of the complex reported in [9b] in which one CO ligand has been replaced by triphenylphosphane [10]. Only very recently the first corresponding dinuclear iron complex of an imine derived from cinnamaldehyde has been isolated and structurally characterised [8g]. Complexes with μ_2-η^3-enyl–amido moieties bridging dinuclear transition metal fragments have been observed as byproducts from the reaction of $Ru_3(CO)_{12}$ with α,β-unsaturated imines of the cinnamaldehyde type [11] and by reacting $[CpCo(C_2H_4)_2]$ with *N*-phenylbenzylideneamine [12]. Related iron compounds of the formula $[(R)N–C(H)–C(H)–Fe(CO)_3–C(O)]Fe(CO)_3$ with a keto group instead of the methylene moiety have been prepared from the reaction of the carbene cluster $(\mu_2\text{-}CH_2)Fe_2(CO)_8$ with phosphine imides in the presence of CO [13]. Thermally induced rearrangement of those binuclear cluster compounds yields the isomeric clusters $[C(H)–C(H)–N(R)–Fe(CO)_3–C(O)]Fe(CO)_3$ [13]. Interestingly the reaction of $Ru_3(CO)_{12}$ with imines derived from benzaldehyde leads to the formation of mononuclear complexes of the general formula $Ru(imine)_2(CO)_2$ in which ruthenium is octahedrally coordinated by the ligands [14] and to a trinuclear ruthenium cluster compound in which the imine is coordinated via the C=N double bond and no C–H activation reaction occurred [14b].

In the first report on a dinuclear iron carbonyl complex with a μ_2-η^3-enyl-amido ligand, the compound was described as an aza-ferra-cyclopentadiene being coordinated to a second $Fe(CO)_3$ moiety in an apical position with two identical iron carbon bond lengths from the aromatic carbon atoms towards the apical iron atom [8f]. The complexes in Refs. [9b,10] show two significantly different iron carbon bond lengths although the only difference is a phenyl group attached to nitrogen instead of a p-toyl substituent in [8f]. In the X-ray structures of thecorresponding complexes derived from heterocyclic imines we also observed this very unsymmetrical coordination of the apical iron atom by the aromatic carbon atoms [8a,b]. So we synthesised six dinuclear iron cluster compounds of the general formula $[\mu_2\text{-}\eta^3\text{-}(R)N–CH_2–C{=}C–C(H){=}C(H)–C(H){=}C(H)]Fe_2(CO)_6$ (Scheme 1) by changing the substituent at nitrogen to see whether the variation of electronic properties also causes changes in the structural properties of these compounds. 2D-NMR experiments of the derivative with $R = C_6H_{11}$ are described in order to explain the NMR properties of the compounds. Since we were particularly interested in the question whether the hydrogen transfer reaction is strictly intramolecular or if there are also intermolecular reaction pathways,

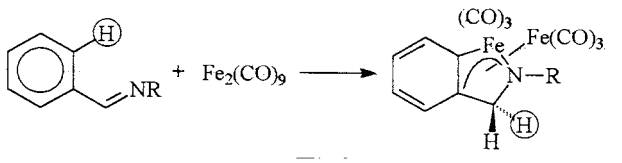

1: R = C_6H_{11}
2: R = C_6H_5
3: R = 4-CH_3-C_6H_4
4: R = 4-Br-C_6H_4
5: R = 4-CF_3-C_6H_4
6: R = 3,5-$(CF_3)_2$-C_6H_3

7: R = C_6H_{11}
8: R = C_6H_5
9: R = 4-CH_3-C_6H_4
10: R = 4-Br-C_6H_4
11: R = 4-CF_3-C_6H_4
12: R = 3,5-$(CF_3)_2$-C_6H_3

Scheme 1.

selectively deuterated ligands and their corresponding cluster compounds have been synthesised. Their ^{1}H- and ^{2}H-NMR spectra indeed show the hydrogen shift reaction to proceed strictly intramolecularly.

2. Results and discussion

The aromatic imine ligands **1**–**6** are easily prepared by condensation of benzaldehyde with the corresponding amine. Reaction of these imine ligands with $Fe_2(CO)_9$ in *n*-heptane at 60°C leads to the formation of the dinuclear iron cluster compounds $[\mu_2\text{-}\eta^3\text{-}N–CH_2–\overline{C{=}C–C(H){=}C(H)–C(H){=}C(H)}]Fe_2(CO)_6$ (**7**–**12**) in moderate yields. Compared to the reaction of heterocyclic imine ligands the yields are distinctively lower [8a,b] (Scheme 1).

2.1. Structural determination

The cluster compounds **7**–**11** may be recrystallised from mixtures of light petroleum (b.p. 40–60°C) and CH_2Cl_2 at −20°C to give crystals suitable for X-ray diffraction. The molecular structure of **7** is shown in Fig. 1; the numbering scheme concerning the cluster

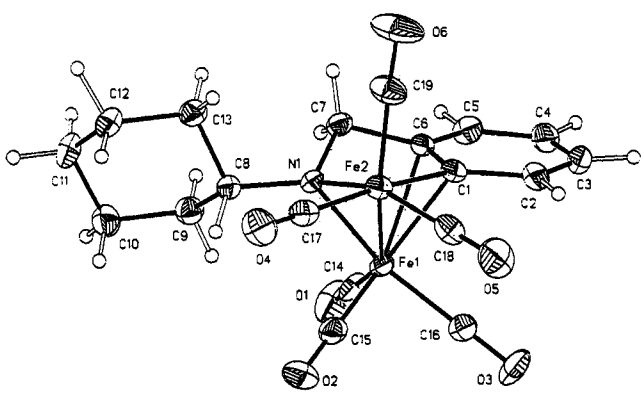

Fig. 1. Molecular structure of $[\mu_2\text{-}\eta^3\text{-}C_6H_{11}–N–CH_2–\overline{C{=}C–C(H){=}C(H)–C(H){=}C(H)}]Fe_2(CO)_6$ (**7**).

Table 1
Selected bond lengths (pm) and angles (°) of **7–11**

	7	**8**	**9**	**10**	**11**
Fe1–Fe2	244.1(1)	246.08(5)	244.54(8)	243.5(1)	244.59(8)
Fe2–C1	198.0(4)	198.7(2)	200.4(2)	198.7(5)	200.6(4)
C1–C6	141.3(6)	141.8(3)	141.4(3)	141.5(7)	140.4(5)
C6–C7	151.0(6)	150.5(3)	149.3(4)	150.5(7)	149.1(5)
N1–C7	147.0(5)	148.4(3)	147.9(3)	149.1(6)	147.8(5)
Fe2–N1	198.8(3)	198.2(2)	198.3(2)	199.4(4)	198.4(3)
C1–C2	144.0(6)	142.7(3)	141.3(3)	142.6(7)	141.9(5)
C2–C3	136.9(7)	136.9(3)	137.4(4)	138.2(9)	136.9(6)
C3–C4	140.5(7)	140.4(4)	139.6(5)	140(1)	139.7(7)
C4–C5	136.4(7)	137.2(3)	135.8(5)	136.5(9)	136.2(6)
C5–C6	141.6(6)	141.2(3)	141.4(3)	142.0(8)	141.2(5)
Fe1–C1	218.1(4)	217.3(2)	216.9(2)	217.8(5)	216.7(4)
Fe1–C6	233.6(4)	231.0(2)	236.9(2)	234.7(5)	237.0(4)
Fe1–N1	197.2(3)	197.0(2)	197.7(2)	197.9(4)	197.5(3)
N1–C8	149.2(5)	143.9(3)	143.8(3)	143.6(6)	144.3(4)
N1–Fe2–C1	78.8(2)	78.80(8)	78.76(9)	79.3(2)	78.3(1)
Fe2–C1–C6	114.2(3)	113.7(1)	112.5(2)	113.6(4)	113.1(3)
C1–C6–C7	113.8(4)	114.2(2)	115.2(2)	114.7(5)	114.8(3)
C6–C7–N1	101.7(3)	101.0(2)	102.0(2)	101.8(4)	102.0(3)
C7–N1–Fe2	111.6(3)	111.4(2)	110.8(1)	110.7(3)	110.7(2)
C1–C2–C3	121.6(4)	121.3(2)	121.3(3)	120.5(6)	121.1(4)
C2–C3–C4	120.7(4)	120.8(2)	120.8(3)	121.5(6)	121.0(4)
C3–C4–C5	120.3(4)	120.2(2)	119.9(3)	120.6(6)	119.9(4)
C4–C5–C6	119.6(4)	119.7(2)	120.3(3)	118.4(6)	119.8(4)
C5–C6–C1	122.0(4)	121.3(2)	120.8(2)	122.9(5)	121.5(4)
C6–C1–C2	115.7(4)	116.7(2)	116.9(2)	116.1(5)	116.8(3)
C7–N1–C8	115.1(3)	115.4(2)	113.1(2)	113.5(4)	112.7(3)
Fe2–N1–C8	122.0(3)	119.0(1)	122.5(2)	122.0(3)	122.4(2)
Fe1–N1–C8	125.4(3)	128.7(1)	127.8(1)	129.4(3)	128.4(2)
Fe2–Fe1–C1	50.4(1)	50.31(5)	51.05(6)	50.7(1)	51.12(9)
Fe2–Fe1–C6	73.7(1)	73.82(5)	72.91(5)	73.5(1)	72.97(8)
Fe2–Fe1–N1	52.2(1)	51.70(5)	51.97(5)	52.5(1)	52.02(8)
C1–Fe1–C6	36.2(2)	36.72(8)	35.97(8)	36.2(2)	35.7(1)
C1–Fe1–N1	74.5(2)	74.70(7)	75.04(8)	75.2(2)	74.8(1)
C6–Fe1–N1	64.3(2)	64.63(7)	63.46(8)	64.3(2)	63.4(1)

core has been adopted for the structure analyses of **8**–**11**. Selected bond lengths and angles are depicted in Table 1. The molecular structure of **8** has been reported in the literature [9b] but has been determined again in order to localise the hydrogen atoms by difference Fourier analysis to prove the formation of a methylene group at C7 which is the former imine carbon atom of the free ligand. In the structure analyses of **7**–**11** all hydrogen atoms have been localised by difference Fourier analyses and have been refined isotropically without constraints.

As shown in Fig. 1, the structure consists of a $Fe_2(CO)_6$ moiety adopting a nearly ecliptic conformation and a formal six-electron donating enyl–amido ligand. The bond lengths and angles in Table 1 indicate that mainly the bond distance between N1 and the ipso atom C8 is affected by the variation of the organic group at the former imine nitrogen atom whereas the other bond lengths and angles show no significant differences. The bond lengths at C7 are clearly single bonds; the bonds inside the metallated phenyl group now are of alternating values, indicating a loss of delocalisation caused by the coordination to the iron atoms. So the bonds C1–C2, C3–C4 and C5–C6 are significantly shorter than the bonds C2–C3 and C4–C5. The bond between C1 and C6 is elongated compared with the distances between C2–C3 and C4–C5 due to a π-coordination to the apical $Fe(CO)_3$ group. This interaction shows a very unsymmetrical bonding mode with the bond between Fe1–C6 always being about 20 pm longer than the Fe1–C1 bond distance. The other bond lengths and angles are of expected values.

2.2. NMR spectroscopy

The most characteristic features in the ^{1}H- and ^{13}C-NMR spectra of **7**–**12** are the signals of the methylene group which was formed during the C–H activation/1,3-hydrogen shift reaction sequence. In the ^{1}H-NMR

spectra a singlet at $\delta = 3.92$ is observed for **7** with R being a cyclohexyl group, whereas the signals in **8–12** with aromatic substituents bound to nitrogen are found at nearly identical chemical shifts at about $\delta = 4.35$. The corresponding ^{13}C resonance is observed at about $\delta = 75$ for the compounds with aromatic substituents bound to nitrogen and at $\delta = 64.8$ for **7**.

In order to achieve an unequivocal assignment of the ^{1}H and especially of the ^{13}C resonances of the metallated phenyl group, several 2D-NMR spectra of **7** have been recorded. Compound **7** was chosen as the model compound since in the ^{1}H-NMR spectrum the remaining four aromatic hydrogen atoms at C2–C5 show four clearly separated signals and in the ^{13}C-NMR spectrum of course only the six resonances for the metallated phenyl group are observed in the downfield region of the spectrum. With the help of a NOESY spectrum of **7** it can be shown that there is a NOE between the resonance of the methylene group and the signal at $\delta = 7.50$ which thus has to be assigned to the proton at C5. The resonance of H5 shows a second NOE crosspeak with the signal at $\delta = 7.32$ which therefore is representing H4. Again there is a second NOE of H4 with the signal at $\delta = 7.07$ which therefore has to be the resonance of H3 and which also shows a second NOE with the doublet at $\delta = 8.12$ which then is the signal of H2. Using this information, the assignment of the ^{13}C spectrum is easily interpreted by means of a HMQC spectrum. This spectrum clearly shows that the ^{13}C resonance at $\delta = 125.6$ represents C3, the one at $\delta = 128.1$ C5, at $\delta = 130.5$ C4 and at $\delta = 151.0$ C2. The two quaternary carbon signals at $\delta = 125.5$ and $\delta = 145.6$, respectively, are assigned by comparing the spectra with those of related μ_2-vinyl complexes in which the resonance of the carbon atom which interacts with both metal centres is observed downfield compared to the signal of the carbon atom which is only part of the π-coordination of the double bond towards one of the metal atoms [15]. So C6 gives rise to a carbon resonance at $\delta = 125.5$ whereas the signal at $\delta = 145.6$ is representing C1. The ^{13}C signals of the metallated phenyl group in **8–12** with aromatic substituents being bound to nitrogen show almost identical chemical shifts, whereas the corresponding resonances of **7** with a alkyl group instead are observed at slightly different values (see Section 3).

2.3. Deuterated ligands and complexes

Scheme 2 shows the synthesis of deuterated ligands and the corresponding dinuclear iron cluster compounds. The ^{2}H-NMR spectrum of **1a** proves the ligand to be selectively deuterated since there is only one signal present at $\delta = 7.78$. If the ligands **1a** and **2a** are reacted with $Fe_2(CO)_9$ the deuterated homologues of **7** and **8** are produced (**7a** and **8a**).

If there was no isotopic effect the two *ortho* positions in **1a** and **2a** should both be activated to the same extend during the reaction with $Fe_2(CO)_9$ and so the product compound should be a 1:1 mixture of two different cluster compounds. In one of them the *ortho* C–H bond would have been activated and thus by 1,3-hydrogen shift a methylene group would have been produced at the former imine carbon atom, whereas the deuterium atom would still adopt its position at the metallated phenyl ring at C5. The other isomer would be produced by activation of the *ortho* C–D bond in **1a** or **2a**, so the product would show a CHD group at the former imine carbon atom and a hydrogen at C5 (Scheme 2). The ^{1}H-NMR spectrum of **7a** shows the signal of H5 at $\delta = 7.46$ with approximately half the intensity compared to the resonances of H4, H3 and H2. In addition the signal representing the methylene group at $\delta = 3.91$ shows an integral representing about 1.5 hydrogen atoms. So the product indeed consists of a 50:50 mixture as it is depicted in Scheme 2. The deuterium-NMR spectrum of **7a** thus shows two signals at $\delta = 3.89$ and $\delta = 7.49$ representing the two possible

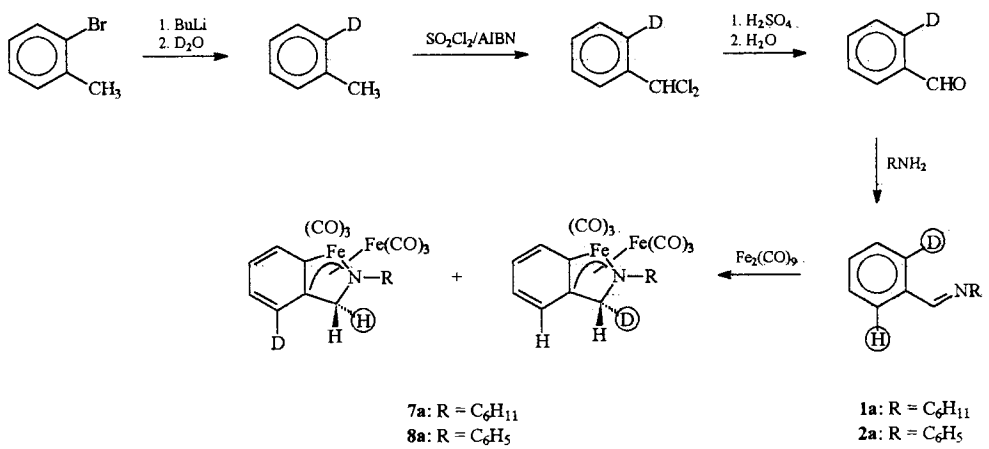

Scheme 2.

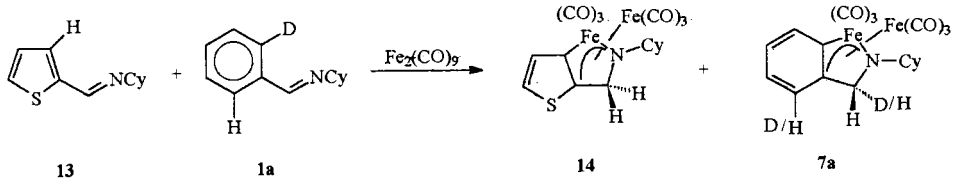

Scheme 3.

positions of deuterium in the molecule. From these ^{1}H- and ^{2}H-NMR spectra of **7a** a scrambling of deuterium towards other positions in the molecule such as the ones shown in Scheme 2 can clearly be excluded. Therefore, it is reasonable that the hydrogen/deuterium atom to be transferred towards the former imine carbon atom is exactly the one that has been connected to the now metallated carbon atom of the phenyl ring before the reaction.

In order to prove whether the hydrogen transfer reaction being responsible for the formation of the methylene group in the dinuclear product clusters **7**–**12** proceeds via an intramolecular pathway we looked at the reaction of $Fe_2(CO)_9$ with **1a** and a heterocyclic imine ligand namely 2-thiophenemethylenecyclohexylamine **13** (Scheme 3). Recently, we reported the reactivity of **13** towards $Fe_2(CO)_9$ leading to derivatives of **7**–**12** [8a].

We chose **13** because in the resulting dinuclear cluster compound **14** the ^{1}H-NMR resonances of the two remaining aromatic protons have the same chemical shift and the signal of the methylene group in the product is well separated from the corresponding resonance of **7a**. In the ^{1}H-NMR spectrum of the product mixture (Fig. 2) the signal of the aromatic hydrogen atoms of **14** is observed at about the same chemical shift as H4 in **7a**, but the resonances of H2, H3 and H5 still are clearly separated. Since the yield of **7a** and **14** may be different we can only compare the intensity of the signals belonging to the same compound. As expected, the intensity of H5 in **7a** is half the intensity of H2 and H3 and the signal of the corresponding methylene group is 1.5 times the intensity of H2 and H3 as it was already shown for pure **7a**. If on the other hand, the intensity of the methylene resonance of **14** represents two protons in **14**, the multiplet at about $\delta = 7.3$ representing the aromatic protons in **14** and H4 in **7a** is exactly the sum of two protons in **14** and one in **7a**. In addition, the ^{2}H-NMR spectrum of the mixture of **7a** and **14** only shows the signals of **7a** but no resonances that would arise from deuterium incorporation in **14** during the formation of the cluster compounds. This result proves that the C–H activation/1,3-hydrogen shift reaction sequence strictly follows an intramolecular pathway since there is also no deuterium scrambling from the deuterated ligand **1a** towards the reaction product of $Fe(CO)_9$ with the thiophene ligand **13**.

3. Experimental

3.1. General

All procedures were carried out under an argon atmosphere in anhydrous, freshly distilled solvents. Chromatography was done using silica gel 60 and silanised silica gel 60, 70–230 mesh ASTM (Merck), which were dried at 10^{-2} bar (10^3 Pa) for 2 days before use. $Fe_2(CO)_9$ was prepared from $Fe(CO)_5$ (Lancaster) by irradiation in acetic acid [16]. Infrared spectra were recorded on a Perkin–Elmer FT-IR System 2000 using 0.2 mm KBr cuvettes. NMR spectra were recorded on a Bruker AC 200 spectrometer (^{1}H: 200 MHz with $SiMe_4$ as internal standard; ^{13}C: 50.32 MHz with $CDCl_3$ as internal standard), ^{1}H, HMQC and NOESY spectra of **7** on a Bruker DRX 400 spectrometer (^{1}H: 400 MHz; ^{13}C: 100.62 MHz with $CDCl_3$ as internal standard), ^{2}H-NMR spectra of **1a**, **7a** and the mixture of **7a** and **14** on a Varian Inova 500 spectrometer (^{2}H: 76.75 MHz). Mass spectra were recorded on a Finnigan MAT SSQ 710 instrument. Elemental analyses were carried out at the laboratory of the Institute of Organic Chemistry and Macromolecular Chemistry of the Friedrich-Schiller-University, Jena.

3.2. X-ray crystallographic studies

Structural determination was carried out on a Siemens P4 diffractometer using graphite monochromated Mo–K_α radiation. The crystals were mounted in a stream of cold nitrogen. Data were corrected for Lorentz and polarisation effects but not for absorption. The structures were solved by direct methods and refined by full-matrix least-squares techniques against F^2 using the programs SHELXS-86 and SHELXL-93 [17]. Computations of the structures were done with the program XPMA [18] and the molecular illustrations were drawn using the program XP [19]. The crystal and intensity data are given in Table 2. Additional material on the structure analyses is available from the Fachinformationszentrum Chemie, Physik, Mathematik GmbH, 76344 Eggenstein-Leopoldshafen 2, Germany by mentioning the deposition numbers CSD-410169 (**7**), -410170 (**8**), -410171 (**9**), -410172 (**10**), -410173 (**11**), the author and the journal citation.

3.3. Preparation of *1–6*

The imines are prepared by stirring 5 g (47.2 mmol) of benzaldehyde with an equimolar amount of the corresponding amine (**1**: R = C_6H_{11}, 4.67 g; **2**: R = C_6H_5, 4.39 g; **3**: R = 4-CH_3–C_6H_4, 5.05 g; **4**: R = 4-Br–C_6H_4, 8.11 g; **5**: R = 4-CF_3–C_6H_4, 7.59 g; **6**: R = 3,5-$(CF_3)_2$–C_6H_3, 10.80 g) at 50°C. The proceeding of the reaction is monitored by GC. After the reaction is finished the resulting yellow to orange coloured oil is distilled in vacuo to yield yellow oils, which crystallise upon standing at room temperature (r.t.). Yields: **1**: R = C_6H_{11}, 7.28 g, 85.3%; **2**: R = C_6H_5, 8.15 g, 92.4%; **3**: R = 4-CH_3–C_6H_4, 9.12 g, 99.2%; **4**: R = 4-Br–C_6H_4, 7.99 g, 65.2%; **5**: R = 4-CF_3–C_6H_4, 11.64 g, 99.1%; **6**: R = 3,5-$(CF_3)_2$–C_6H_3, 11.90 g, 79.6%. The identity and purity of **1**–**4** is confirmed by comparison of the boiling points and the NMR spectra with the data reported in the literature [20].

3.3.1. MS and spectroscopical data for *5*

MS (EI): *m*/*z* (%) 249 (M^+, 90), 248 ($M^+ - H$, 100), 230 ($M^+ - F$, 10), 180 ($M^+ - CF_3$, 7), 172 ($C_8H_5NF_3^+$, 13), 152 ($C_{12}H_8^+$, 8), 145 ($C_7H_4F_3^+$, 63), 125 ($C_7H_3F_2^+$, 11), 105 ($C_7H_2F^+$, 11), 95 ($C_7H_5^+$, 17), 77 ($C_6H_5^+$, 26), 63 ($C_5H_3^+$, 7), 51 ($C_4H_3^+$, 13), 39 ($C_3H_3^+$, 13); ^{1}H-NMR (in $CDCl_3$, 298 K) (ppm): 7.18–7.22 (m, 2 H, =CH), 7.39–7.55 (m, 3 H, =CH), 7.57–7.61 (m, 2 H, =CH), 7.84–7.89 (m, 2 H, =CH), 8.36 (s, 1 H, N=CH); ^{13}C-NMR (in $CDCl_3$, 298 K) (ppm): 121.0 (=CH), 124.4 (CF_3, $^1J_{CF} = 272$ Hz), 126.4 (=CH, $^3J_{CF} = 4$ Hz), 127.8 (=C, $^2J_{CF} = 33$ Hz), 128.8 (=CH), 129.1 (=CH), 132.4 (=CH), 135.8 (=C), 155.2 (=C), 161.9 (N=CH).

3.3.2. MS and spectroscopical data for *6*

MS (EI): *m*/*z* (%) 317 (M^+, 69), 316 ($M^+ - H$, 100), 248 ($C_{14}H_9NF_3^+$, 7), 240 ($C_9H_4NF_6^+$, 8), 229 ($C_{14}H_9NF_2^+$, 11), 213 ($C_8H_3F_6^+$, 35), 182 ($C_7H_3F_5^+$, 3), 163 ($C_7H_3F_4^+$, 8), 122 ($C_7H_5NF^+$, 11), 104 ($C_7H_6N^+$, 15), 89 ($C_7H_5^+$, 8) 77 ($C_6H_5^+$, 39), 63 ($C_5H_3^+$, 5), 51 ($C_4H_3^+$, 11), 39 ($C_3H_3^+$, 4); ^{1}H-NMR (in $CDCl_3$, 298 K) (ppm): 7.31–7.47 (m, 3 H, =CH), 7.53 (s, br, 2 H, =CH), 7.67 (s, br, 1 H, =CH), 7.79–7.87 (m, 2 H, =CH), 8.32 (s, 1 H, N=CH); ^{13}C-NMR (in $CDCl_3$, 298 K) (ppm): 119.1 (=CH, $^3J_{CF} = 4$ Hz), 121.1 (=CH, $^4J_{CF} = 3$ Hz), 128.1 (CF_3, $^1J_{CF} = 206$ Hz), 128.9 (=CH), 129.5 (=CH), 132.4 (=CH), 133.3 (=C, $^2J_{CF} = 33$ Hz), 135.4 (=C), 153.5 (=C), 163.1 (N=CH).

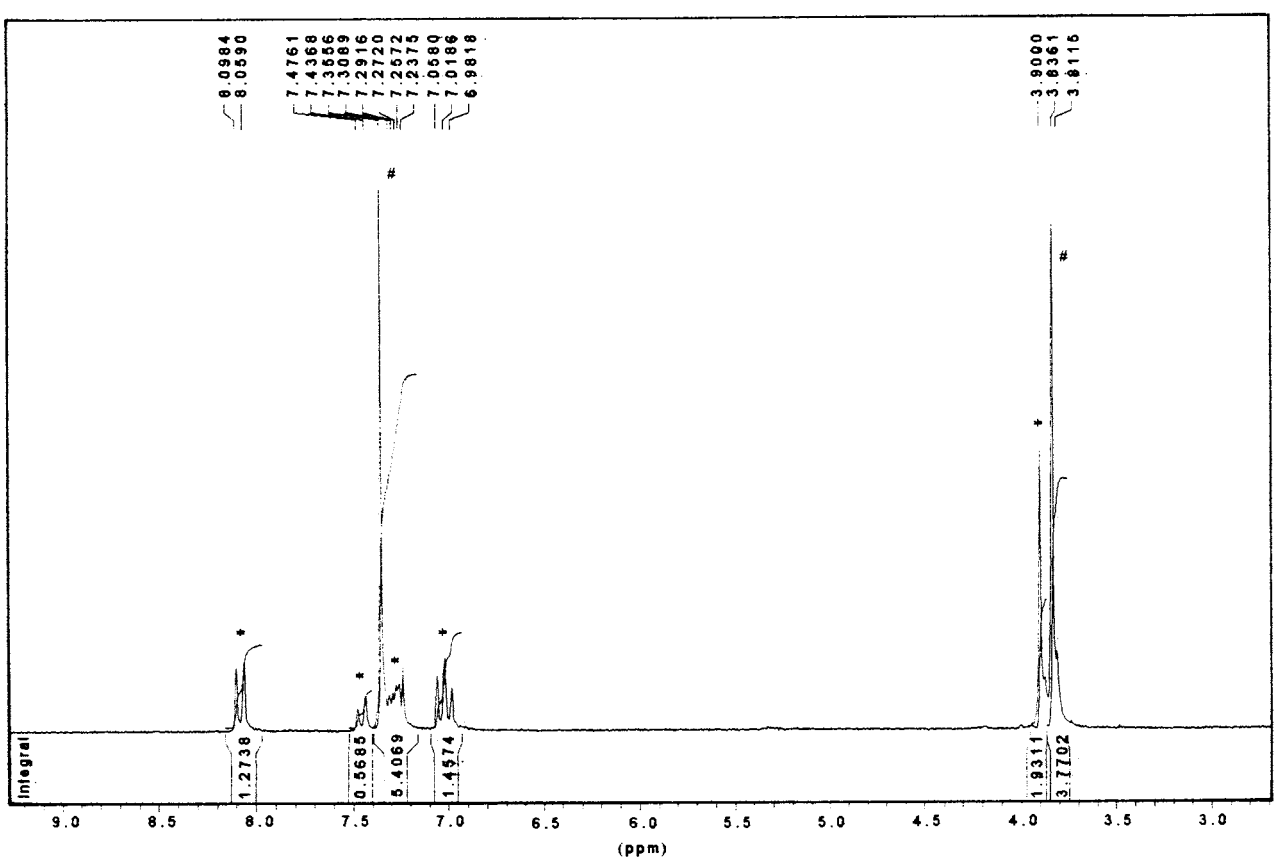

Fig. 2. ^{1}H-NMR spectrum of a mixture of **7a** (*) and **14** (#); cyclohexyl signals are not shown.

Table 2
Crystal and intensity data for compounds **7–11**

	7	**8**	**9**	**10**	**11**
Formula	$C_{19}H_{17}NO_6Fe_2$	$C_{19}H_{11}NO_6Fe_2$	$C_{20}H_{13}NO_6Fe_2$	$C_{19}H_{10}BrNO_6Fe_2$	$C_{20}H_{10}F_3NO_6Fe_2$
Molecular weight (g mol^{-1})	467.04	460.99	475.01	539.89	528.99
Radiation	Mo–K_α	Mo–K_α	Mo–K_α	Mo–K_α	Mo–K_α
Monochromator	Graphite	Graphite	Graphite	Graphite	Graphite
Temperature (K)	213	213	213	213	213
Crystal colour	Red	Red	Red	Red	Red
Crystal size (mm)	$0.4\times0.4\times0.3$	$0.4\times0.4\times0.4$	$0.6\times0.4\times0.2$	$0.5\times0.3\times0.05$	$0.3\times0.3\times0.2$
a (Å)	26.182(6)	7.568(1)	12.684(4)	12.675(4)	13.227(2)
b (Å)	8.337(2)	8.363(1)	11.824(3)	11.746(2)	11.535(2)
c (Å)	17.802(5)	15.435(2)	13.582(4)	13.400(3)	13.831(5)
α (°)	90	77.702(8)	90	90	90
β (°)	97.91(2)	78.331(9)	104.08(2)	94.26(2)	104.90(2)
γ (°)	90	80.16(1)	90	90	90
Volume (Å^3)	3849(2)	926.4(2)	1975(1)	1989.5(8)	2039.3(9)
Z	8	2	4	4	4
$F(000)$	1904	464	960	1064	1056
D_{calc} (g cm^{-3})	1.612	1.653	1.597	1.802	1.723
Crystal system	Monoclinic	Triclinic	Monoclinic	Monoclinic	Monoclinic
Space group	$C2/c$	$P\bar{1}$	$P2_1/n$	$P2_1/c$	$P2_1/c$
Absorption coefficient (mm^{-1})	1.789	1.606	1.509	3.506	1.492
θ Limit	1.57–26.02	1.37–25.00	1.97–27.49	2.13–27.50	1.90–24.99
Scan mode	θ–2θ	θ–2θ	θ–2θ	θ–2θ	θ–2θ
Scan speed (° min^{-1})	3–60	3–60	3–60	3–60	3–60
No. reflections measured	4631	4028	4513	5652	4535
Independent reflections	3782	3227	4513	4550	3596
R_{int}	0.0359	0.0129	0.0000	0.0300	0.0318
No. observed reflections $F_o^2 = 2\sigma(F_o^2)$	2760	2938	3857	3123	2840
No. of parameters	321	297	304	302	329
GOF	1.026	0.981	1.036	1.035	1.097
R_1	0.0500	0.0256	0.0367	0.0626	0.0409
wR_2	0.1189	0.0651	0.0949	0.1491	0.0950
Final difference map electron density (e Å^{-3})	0.894	0.233	0.521	1.355	0.675

3.4. Preparation of 7–12

A 500 mg (1.4 mmol) sample of $Fe_2(CO)_9$ was stirred together with 1.2 equivalents of the corresponding imine (**7**: R = C_6H_{11}, 308 mg; **8**: R = C_6H_5, 298 mg; **9**: R = 4-CH_3–C_6H_4, 321 mg; **10**: R = 4-Br–C_6H_4, 429 mg; **11**: R = 4-CF_3–C_6H_4, 410 mg; **12**: R = 3,5-$(CF_3)_2$–C_6H_3, 523 mg) in 30 ml *n*-heptane at 50°C. During the reaction the colour of the solution changes from orange to deep red and the undissolved $Fe_2(CO)_9$ slowly disappears. After 1 h all of the starting material is dissolved and the solvent is evaporated in vacuo. The resulting oily residue is dissolved in 10 ml CH_2Cl_2 and 1 g silanised silica gel is added. Chromatography in all cases first yields a green fraction of $Fe_3(CO)_{12}$ using a mixture of light petroleum (b.p. 40–60°C)/CH_2Cl_2 10:1 and a second red coloured band of **7**–**12** using a mixture of light petroleum/CH_2Cl_2 4:1 (yields: 222 mg **7**, 34%; 181 mg **8**, 28%; 140 mg **9**, 21%; 136 mg **10**, 18%; 178 mg **11**, 24%; 184 mg **12**, 22%). If the reaction mixture producing **10** is stirred at r.t. instead of being heated the formation of $Fe_3(CO)_{12}$ is reduced and the yield of **10** improves to 32%. Compounds **7**–**12** are recrystallised from a mixture of light petroleum/CH_2Cl_2 at −20°C.

7: m.p. 109°C; $C_{19}H_{17}NO_6Fe_2$; Anal. Found (Calc.) C: 48.79 (48.86), H: 3.71 (3.67), N: 3.00 (3.00)%.

8: m.p. 89°C; $C_{19}H_{11}NO_6Fe_2$; Anal. Found (Calc.) C: 49.44 (49.50), H: 2.45 (2.41), N: 3.04 (3.04)%.

9: m.p. 102°C; $C_{20}H_{13}NO_6Fe_2$; Anal. Found (Calc.) C: 50.82 (50.57), H: 2.99 (2.76), N: 2.94 (2.95)%.

10: m.p. 140°C; $C_{19}H_{10}BrNO_6Fe_2$; Anal. Found (Calc.) C: 42.50 (42.27), H: 1.85 (1.87), N: 2.64 (2.59)%.

11: m.p. 107°C; $C_{20}H_{10}F_3NO_6Fe_2$; Anal. Found (Calc.) C: 45.33 (45.41), H: 2.02 (1.91), N: 2.60 (2.65)%.

12: m.p. 93°C; $C_{21}H_9F_6NO_6Fe_2$; Anal. Found (Calc.) C: 41.97 (42.25), H: 1.58 (1.52), N: 2.31 (2.35)%.

3.4.1. MS and spectroscopical data for 7

MS (EI): *m*/*z* (%) 467 (M^+, 5), 439 ($M^+ - CO$, 3), 411 ($M^+ - 2CO$, 16), 383 ($M^+ - 3CO$, 13), 355 ($M^+ - 4CO$, 19), 327 ($M^+ - 5CO$, 85), 299 ($M^+ - 6CO$, 100), 237 ($C_8H_{11}NFe_2^+$, 41), 215 ($C_{11}H_{13}NFe^+$, 24), 203 ($C_{10}H_{13}NFe^+$, 6), 190 ($C_9H_{12}NFe^+$, 9), 178

($C_8H_{12}NFe^+$, 24), 164 ($C_7H_{10}NFe^+$, 28), 148 ($C_6H_6NFe^+$, 46), 135 ($C_5H_5NFe^+$, 35), 112 (Fe_2^+, 70), 91 ($C_7H_7^+$, 26), 84 ($C_6H_{12}^+$, 8), 56 (Fe^+, 53); IR (in CH_2Cl_2, 298 K) (cm^{-1}): 2060 (m), 2023 (vs), 1979 (br); ^{1}H-NMR (in $CDCl_3$, 298 K) (ppm): 1.04–1.87 (m, 10 H, CH_2), 2.30–2.32 (m, 1 H, CH), 3.95 (s, 2 H, CH_2), 7.07 (ddd, 1 H, =CH, $^3J_{HH} = 8.1$ Hz, $^3J_{HH} = 6.9$ Hz, $^4J_{HH} = 1.3$ Hz), 7.32 (ddd, 1 H, =CH, $^3J_{HH} = 8.1$ Hz, $^3J_{HH} = 6.9$ Hz, $^4J_{HH} = 1.1$ Hz), 7.50 (dd, 1 H, =CH, $^3J_{HH} = 8.1$ Hz, $^4J_{HH} = 1.3$ Hz), 8.12 (dd, 1 H, =CH, $^3J_{HH} = 8.1$ Hz, $^4J_{HH} = 1.1$ Hz); ^{13}C-NMR (in $CDCl_3$, 298 K) (ppm): 26.1 (CH_2), 26.2 (CH_2), 35.4 (CH_2), 64.8 (CH_2), 74.2 (CH), 125.5 (=C), 125.6 (=CH), 128.1 (=CH), 130.5 (=CH), 145.6 (=C), 151.0 (=CH), 210.6 (CO).

3.4.2. MS and spectroscopical data for **8**

MS (EI): m/z (%) 461 (M^+, 7), 433 ($M^+ - CO$, 3), 405 ($M^+ - 2CO$, 18), 377 ($M^+ - 3CO$, 13), 349 ($M^+ - 4CO$, 24), 321 ($M^+ - 5CO$, 52), 293 ($M^+ - 6CO$, 100), 237 ($C_{13}H_{11}NFe^+$, 60), 159 ($C_7H_5NFe^+$, 24), 147 ($C_6H_5NFe^+$, 70), 133 ($C_5H_3NFe^+$, 23), 112 (Fe_2^+, 21), 77 ($C_6H_5^+$, 9), 56 (Fe^+, 50); IR (in CH_2Cl_2, 298 K) (cm^{-1}): 2066 (m), 2028 (vs), 1987 (br); ^{1}H-NMR (in $CDCl_3$, 298 K) (ppm): 4.36 (s, 2 H, CH_2), 7.03–7.34 (m, 7 H, =CH), 7.56–7.60 (m, 1 H, =CH), 8.01–8.05 (m, 1 H, =CH); ^{13}C-NMR (in $CDCl_3$, 298 K) (ppm): 75.3 (CH_2), 120.7 (=C), 122.8 (=CH), 125.4 (=CH), 126.0 (=CH), 128.9 (=CH), 129.3 (=CH), 129.9 (=CH), 149.3 (=C), 150.1 (=CH), 158.8 (=C), 210.4 (CO).

3.4.3. MS and spectroscopical data for **9**

MS (EI): m/z (%) 475 (M^+, 7), 447 ($M^+ - CO$, 1), 419 ($M^+ - 2CO$, 15), 391 ($M^+ - 3CO$, 16), 363 ($M^+ - 4CO$, 26), 335 ($M^+ - 5CO$, 57), 307 ($M^+ - 6CO$, 100), 278 ($C_{13}H_{10}Fe_2^+$, 2), 251 ($C_{14}H_{13}NFe^+$, 51), 224 ($C_{12}H_{10}NFe^+$, 11), 194 ($C_{11}H_6Fe^+$, 11), 173 ($C_8H_7NFe^+$, 15), 154 ($C_2H_4NFe_2^+$, 50) 112 (Fe_2^+, 17), 91 ($C_7H_7^+$, 11), 56 (Fe^+, 32); IR (in CH_2Cl_2, 298 K) (cm^{-1}): 2065 (m), 2027 (vs), 1987 (br); ^{1}H-NMR (in $CDCl_3$, 298 K) (ppm): 2.29 (s, 3 H, CH_3), 4.34 (s, 2 H, CH_2), 6.92–7.12 (m, 5 H, =CH), 7.26–7.34 (m, 1 H, =CH), 7.56–7.60 (m, 1 H, =CH), 8.01–8.04 (m, 1 H, =CH); ^{13}C-NMR (in $CDCl_3$, 298 K) (ppm): 20.7 (CH_3), 75.5 (CH_2), 120.7 (=C), 122.6 (=CH), 126.0 (=CH), 129.3 (=CH), 129.4 (=CH), 129.8 (=CH), 135.1 (=C), 149.3 (=C), 150.1 (=CH), 156.4 (=C), 210.4 (CO).

3.4.4. MS and spectroscopical data for **10**

MS (EI): m/z (%) 539 (M^+, 7), 511 ($M^+ - CO$, 3), 483 ($M^+ - 2CO$, 15), 455 ($M^+ - 3CO$, 11), 427 ($M^+ - 4CO$, 18), 399 ($M^+ - 5CO$, 16), 371 ($M^+ - 6CO$, 47), 315 ($C_{13}H_{10}NBrFe^+$, 5), 235 ($C_{13}H_9NFe^+$, 100), 209 ($C_{11}H_7NFe^+$, 35), 180 ($C_{10}H_4Fe^+$, 47), 152 ($C_3H_4Fe_2^+$, 52), 132 ($C_6H_4Fe^+$, 32), 56 (Fe^+, 87); IR (in CH_2Cl_2, 298 K) (cm^{-1}): 2067 (m), 2029 (vs), 1989 (br); ^{1}H-NMR (in $CDCl_3$, 298 K) (ppm): 4.31 (s, 2 H, CH_2), 6.88–6.93 (m, 2 H, =CH), 7.05–7.12 (m, 1 H, =CH), 7.27–7.35 (m, 3 H, =CH), 7.56–7.60 (m, 1 H, =CH), 8.00–8.03 (m, 1 H, =CH); ^{13}C-NMR (in $CDCl_3$, 298 K) (ppm): 75.0 (CH_2), 118.3 (=C), 120.6 (=C), 124.4 (=CH), 126.2 (=CH), 129.4 (=CH), 130.0 (=CH), 132.0 (=CH), 149.1 (=C), 150.2 (=CH), 158.0 (=C), 210.2 (CO).

3.4.5. MS and spectroscopical data for **11**

MS (EI): m/z (%) 529 (M^+, 3), 501 ($M^+ - CO$, 1), 473 ($M^+ - 2CO$, 12), 445 ($M^+ - 3CO$, 7), 417 ($M^+ - 4CO$, 12), 389 ($M^+ - 5CO$, 17), 361 ($M^+ - 6CO$, 68), 286 ($C_8H_7NF_3Fe_2^+$, 6), 267 ($C_8H_7NF_2Fe_2^+$, 7), 247 ($C_5H_4NF_3Fe_2^+$, 11), 240 ($C_9H_5NF_3Fe^+$, 12), 230 ($C_8H_7NF_3Fe^+$, 13), 192 ($C_5H_5NF_3Fe^+$, 100), 165 ($C_4H_4F_3Fe^+$, 76), 91 ($C_7H_7^+$, 10), 89 ($C_7H_5^+$, 17), 56 (Fe^+, 24); IR (in CH_2Cl_2, 298 K) (cm^{-1}): 2068 (m), 2030 (vs), 1990 (br); ^{1}H-NMR (in $CDCl_3$, 298 K) (ppm): 4.35 (s, 2 H, CH_2), 7.07–7.13 (m, 3 H, =CH), 7.29–7.36 (m, 1 H, =CH), 7.47–7.51 (m, 2 H, =CH), 7.59–7.63 (m, 1 H, =CH), 8.00–8.04 (m, 1 H, =CH); ^{13}C-NMR (in $CDCl_3$, 298 K) (ppm): 74.4 (CH_2), 120.2 (=C), 122.8 (=CH), 123.8 (CF_3, $^1J_{CF} = 265$ Hz), 126.3 (=CH, $^3J_{CF} = 3$ Hz), 126.4 (=CH), 126.8 (=CH, $^2J_{CF} = 23$ Hz), 129.6 (=CH), 130.1 (=CH), 149.2 (=C), 150.1 (=CH), 161.8 (=C), 210.1 (CO).

3.4.6. MS and spectroscopical data for **12**

MS (EI): m/z (%) 597 (M^+, 17), 569 ($M^+ - CO$, 3), 541 ($M^+ - 2CO$, 27), 513 ($M^+ - 3CO$, 14), 485 ($M^+ - 4CO$, 14), 457 ($M^+ - 5CO$, 7), 429 ($M^+ - 6CO$, 89), 335 ($C_{12}H_7NF_6Fe^+$, 14), 318 ($C_{11}H_3NF_3Fe_2^+$, 19), 240 ($C_9H_5NF_3Fe^+$, 100), 222 ($C_9H_6NF_2Fe^+$, 35), 214 ($C_7H_3NF_3Fe^+$, 33), 190 ($C_5H_3NF_3Fe^+$, 19), 163 ($C_4H_2F_3Fe^+$, 24), 128 ($C_9H_6N^+$, 39), 112 (Fe_2^+, 9), 91 ($C_7H_7^+$, 27), 76 ($C_6H_4^+$, 11), 56 (Fe^+, 18); IR (in CH_2Cl_2, 298 K) (cm^{-1}): 2070 (m), 2033 (vs), 1993 (br); ^{1}H-NMR (in $CDCl_3$, 298 K) (ppm): 4.37 (s, 2 H, CH_2), 7.09–7.17 (m, 1 H, =CH), 7.32–7.40 (m, 1 H, =CH), 7.42 (s, 2 H, =CH), 7.58 (s, 1 H, =CH), 7.61–7.65 (m, 1 H, =CH), 8.01–8.04 (m, 1 H, =CH); ^{13}C-NMR (in $CDCl_3$, 298 K) (ppm): 74.0 (CH_2), 118.7 (=CH, $^3J_{CF} = 4$ Hz), 120.4 (=C), 122.5 (=CH, $^4J_{CF} = 3$ Hz), 122.8 (CF_3, $^1J_{CF} = 273$ Hz), 126.6 (=CH), 129.6 (=CH), 130.4 (=CH), 132.7 (=CH, $^2J_{CF} = 34$ Hz), 148.6 (=C), 150.3 (=CH), 160.4 (=C), 209.8 (CO).

3.5. 2-Lithiotoluene

A total of 73.0 ml (117 mmol) of a 1.6 N solution of butyllithium in hexane is added to a solution of 20.0 g (117 mmol) of 2-bromotoluene in 150 ml diethylether at −60°C. The reaction mixture is allowed to warm to r.t.

and is stirred another 15 min. Then diethylether is evaporated until only 20 ml are left and 70 ml hexane are added. After standing overnight at −30°C 2-lithiotoluene which is free of diethylether has precipitated as a white solid which is filtered and dried in vacuo. Yield: 16.5 g (81%); m.p. >120°C (dec.).

3.6. 2-Deuterotoluene

To a solution of 16.5 g (168 mmol) of 2-lithiotoluene in 100 ml diethylether 3.35 g (168 mmol) of D_2O are added dropwise at −30°C. After 1 h of stirring the reaction mixture is distilled using a Vigreux column. Yield: 13.1 g (84%); b.p. 110°C; ^{1}H-NMR (in $CDCl_3$, 298 K) (ppm): 2.38 (s, 3 H, CH_3), 7.13–7.35 (m, 4 H, =CH).

3.7. 2-Deuterobenzylidenedichloride

A 13.1 g (81 mmol) sample of 2-deuterotoluene is refluxed together with 22.0 g (162 mmol) SO_2Cl_2 and 80 mg AIBN. Each hour another 80 mg of AIBN is added. After 20 h the mixture is cooled to r.t., dissolved in 100 ml diethylether, dried with magnesium sulfate and distilled using a Vigreux column. Yield: 12.5 g (55%); b.p. 86°C/1.9 torr; ^{1}H-NMR (in $CDCl_3$, 298 K) (ppm): 6.70 (s, 1 H, $CHCl_2$), 7.27–7.41 (m, 4 H, =CH).

3.8. 2-Deuterobenzaldehyde

A total of 12.5 g (77 mmol) of 2-deuterobenzylidenedichloride is treated with 100 g of concentrated sulphuric acid at 0°C in a two-neck vessel with a reflux condenser and a capillary through which a stream of nitrogen is bubbled through the reaction mixture. At the top of the reflux condenser a water-jet vacuum is applied. The reaction mixture turns reddish brown. After 2 h the reaction mixture is poured on ice and is washed three times with diethylether. The combined diethylether extracts are neutralised with $NaHCO_3$, dried with $MgSO_4$ and after evaporation of the solvent distilled in vacuo. The mass spectrum of the product shows that the degree of deuteration is above 99%. Yield: 5.0 g (61%); b.p. 64°C/1.7 torr; MS (EI): m/z (%) 107 (M^+, 99), 106 ($M^+ - H$, 100), 78 ($C_6H_4D^+$, 88), 52 ($C_4H_2D^+$, 11), 51 (C_4HD^+, 23); ^{1}H-NMR (in $CDCl_3$, 298 K): 7.46–7.65 (m, 3 H, =CH), 7.86 (d, 1 H, $^3J_{HH} = 7.8$ Hz, =CH), 10.00 (s, 1 H, CHO); ^{13}C-NMR (in $CDCl_3$, 298 K): 128.8 (=CH), 129.0 (=CH), 129.4 (t, $^1J_{CD} = 23.9$ Hz, CD), 129.7 (=CH), 134.4 (=CH), 136.4 (=C), 192.3 (CHO).

3.9. Preparation of **1a** and **2a**

A 1.90 g (17.7 mmol) sample of 2-deuterobenzaldehyde in 5 ml ethanol is treated with 1.76 (17.7 mmol) cyclohexylamine and a catalytic amount of *p*-toluenesulfonic acid. The resulting water is trapped by 1 g molecular sieve. After stirring overnight at 70°C the solution is filtered, the solvent is evaporated in vacuo and the yellow oily residue is distilled using a short Vigreux column. In an analogous procedure, 1.10 g (10.3 mmol) of 2-deuterobenzaldehyde was reacted with 0.96 g (10.3 mmol) aniline. The resulting pale yellow imines **1a** and **2a** are recrystallised from ethanol/hexane at −30°C. Yields: **1a**: 2.88 g (86%), b.p. 110–130°C/2.5 torr, m.p. 12°C; **2a**: 1.39 g (77%), b.p. 120–150°C/2.5 torr, m.p. 44°C.

3.9.1. MS and spectroscopical data for **1a**

MS (EI): m/z (%) 188 (100, M^+), 187 (100, $M^+ - H$), 159 (96, $M^+ - C_2H_5$), 145 (87, $M^+ - C_3H_7$), 133 (47, $M^+ - C_4H_7$), 131 (23, $M^+ - C_4H_9$), 105 (91, $M^+ - C_6H_{11}$), 92 (23, $C_7H_6D^+$), 91 (22, $C_7H_7^+$), 78 (19, $C_6H_4D^+$), 77 (8, $C_6H_5^+$), 55 (35, $C_4H_7^+$), 41 (32, $C_3H_5^+$); IR (298 K) (cm^{-1}): 1643 (vs, C=N); ^{1}H-NMR (in $CDCl_3$, 298 K): 1.10–1.90 (m, 10 H, CH_2), 3.05–3.28 (m, 1 H, CH), 7.38–7.40 (m, 3 H, =CH), 7.68–7.76 (m, 1 H, =CH), 8.31 (s, 1 H, CH=N); ^{2}H-NMR (in $CHCl_3$, 298 K): 7.73 (s, =CD); ^{13}C-NMR (in $CDCl_3$, 298 K): 23.3 (CH_2), 24.9 (CH_2), 34.3 (CH_2), 69.8 (CH), 127.7 (t, $^1J_{CD} = 24.2$ Hz, =CD), 128.0 (=CH), 128.3 (=CH), 128.4 (=CH), 130.2 (=C), 158.4 (CH=N).

3.9.2. MS and spectroscopical data for **2a**

MS (EI): m/z (%) 182 (85, M^+), 181 (100, $M^+ - H$), 104 (12, $M^+ - C_6H_5$), 77 (57, $C_6H_5^+$), 51 (17, $C_4H_3^+$); IR (KBr, 298 K) (cm^{-1}): 1703 (vs, C=N); ^{1}H-NMR (in $CDCl_3$, 298 K): 7.20–7.55 (m, 8 H, =CH), 7.85–7.98 (m, 1 H, =CH), 8.47 (s, 1 H, CH=N); ^{13}C-NMR (in $CDCl_3$, 298 K): 120.8 (=CH), 125.9 (=CH), 128.5 (t, $^1J_{CD} = 24.2$ Hz, =CD), 128.6 (=CH), 128.7 (=CH), 129.0 (=CH), 129.7 (=CH), 136.2 (=C), 152.1 (=C), 160.3 (CH=N).

3.10. Preparation of **7a** and **8a**

A total of 500 mg (1.37 mmol) $Fe_2(CO)_9$ is suspended in 30 ml hexane together with an equimolar amount of the corresponding imine (**1a**: 260 mg, **2a**: 250 mg). After 2 h of stirring at 50°C the solution turns red and the solvent is evaporated in vacuo. The residue is dissolved in 5 ml CH_2Cl_2 and 1 g silanised silica gel is added. After removing CH_2Cl_2 the product mixture is chromatographed. Compounds **7a** and **8a** are eluted using a mixture of light petroleum (b.p. 40–60°C)/CH_2Cl_2 20:1 as a deep red coloured band. The solutions of **7a** and **8**a are evaporated until only a few ml of solvent is left and crystallised overnight at −30°C. Yields: **7a**: 265 mg (41%), m.p. 108°C, $C_{19}H_{16}DFe_2NO_6$ (468.06): Calc. C 48.75, N 2.99; found C 48.76, N 2.90; **8a**: 230 mg (36%), m.p. 91°C, $C_{19}H_{10}DFe_2NO_6$ (462.00) Calc.: C,

49.39; N, 3.03; Found: C, 49.37; N, 2.96%. Analytical values for hydrogen are not given since the instrument used for CHN-analysis cannot determine D_2O quantitatively.

3.10.1. MS and spectroscopical data for ***7a***

MS (EI): *m/z* (%) 468 (M^+, 32), 440 ($M^+ - CO$, 17), 412 ($M^+ - 2CO$, 100), 384 ($M^+ - 3CO$, 17), 356 ($M^+ - 4CO$, 22), 328 ($M^+ - 5CO$, 80), 300 ($M^+ - 6CO$, 100), 244 ($M^+ - 6CO - Fe$, 10), 238 ($C_8H_{10}DNFe_2^+$ or $C_8H_{12}NFe_2^+$, 26), 216 ($C_{11}H_{12}DNFe^+$ or $C_{11}H_{14}NFe^+$, 14), 149 ($C_6H_5DNFe^+$ or $C_6H_7NFe^+$, 33), 134 ($C_5H_4NFe^+$, 12), 112 (Fe_2^+, 24), 56 (Fe^+, 18); IR (Nujol, 298 K) (cm^{-1}): 2060 (s), 2023 (s), 1983 (s); ^{1}H-NMR (in $CDCl_3$, 298 K): 0.80–1.90 (m, 10 H, CH_2), 2.23–2.34 (m, 1 H, CH), 3.91 (s, 1.5 H, CH_2/CHD), 7.03 (t, $^3J_{HH} = 7.5$ Hz, 1 H, =CH), 7.25–7.32 (m, 1 H, =CH), 7.46 (d, $^3J_{HH} = 8.1$ Hz, 0.5 H, =CH), 8.09 (d, $^3J_{HH} = 8.1$ Hz, 1 H, =CH); ^{2}H-NMR (in $CHCl_3$, 298 K): 3.89 (s, CHD), 7.49 (s, =CD); ^{13}C-NMR (in $CDCl_3$, 298 K): 26.0 (CH_2), 26.2 (CH_2), 35.4 (CH_2), 64.4 (t, $^1J_{CD} = 23.2$ Hz, CHD), 64.7 (CH_2), 74.2 (CH), 125.1 (=C, *ortho* to =CH or =CD), 125.2 (=C, *ortho* to =CH or =CD), 125.6 (=CH), 128.1 (=CH), 130.4 (=CH, *ortho* to =CH or =CD), 130.5 (=CH, *ortho* to =CH or =CD), 145.6 (=C), 150.9 (=CH), 210.6 (CO), the expected triplet representing the deuterated aromatic carbon atom has not been observed.

3.10.2. MS and spectroscopical data for ***8a***

MS (EI): *m/z* (%) 462 (M^+, 5), 434 ($M^+ - CO$, 1), 406 ($M^+ - 2CO$, 20), 378 ($M^+ - 3CO$, 17), 350 ($M^+ - 4CO$, 29), 322 ($M^+ - 5CO$, 58), 294 ($M^+ - 6CO$, 100), 238 ($M^+ - 6CO - Fe$, 69), 159 ($C_7H_3DNFe^+$ or $C_7H_5NFe^+$, 14), 147 ($C_6H_3DNFe^+$ or $C_6H_5NFe^+$, 51), 112 (Fe_2^+, 14), 56 (Fe^+, 29); IR (Nujol, 298 K) (cm^{-1}): 2066 (s), 2027 (s), 1993 (s), 1983 (s); ^{1}H-NMR (in $CDCl_3$, 298 K): 4.37 (s, 1.5 H, CH_2/CHD), 7.06–7.24 (m, 7 H, =CH), 7.58 (d, $^3J_{HH} = 8.2$ Hz, 0.5 H, =CH), 8.03 (d, $^3J_{HH} = 8.2$ Hz, 1 H, =CH); ^{13}C-NMR (in $CDCl_3$, 298 K): 74.8 (t, $^1J_{CD} = 18.2$ Hz, CHD), 75.2 (CH_2), 120.4 (=C), 125.4 (=CH), 126.0 (=CH), 128.9 (=CH), 129.4 (=CH), 129.7 (=CH), 129.8 (=CH), 149.4 (=C), 150.1 (=C), 158.7 (=C), 210.4 (CO), the expected triplet representing the deuterated aromatic carbon atom has not been observed.

Acknowledgements

We thank the Deutsche Forschungsgemeinschaft (SFB 436) for financial support and Dr. W. Günther, Institute of Organic Chemistry and Macromolecular Chemistry, Friedrich-Schiller-University, Jena for the NOESY and HMQC spectra of **7**.

References

[1] (a) M. Brookhart, M.L.H. Green, J. Organomet. Chem. 250 (1983) 395. (b) E.C. Constable, Polyhedron 3 (1984) 1037. (c) J. Halpern, Inorg. Chim. Acta 100 (1985) 41. (d) R.H. Crabtree, Chem. Rev. 85 (1985) 245. (e) A.D. Ryabov, Chem. Rev. 90 (1990) 403. (f) J.A. Davies Ed., Selective Hydrocarbon Activation, VCH, Weinheim, 1990. (g) B.A. Arndtsen, R.G. Bergman, T.A. Mobley, T.H. Petersen, Acc. Chem. Res. 28 (1995) 154. (h) R.H. Crabtree, Chem. Rev. 95 (1995) 987. (i) Y. Fujiwara, K. Takagi, Y. Taniguchi, Synlett (1996) 591.

[2] (a) Ketones: M. Sonoda, F. Kakiuchi, N. Chatani, S. Murai, Bull. Chem. Soc. Jpn. 70 (1997) 3117 and literature cited therein. (b) Imines: F. Kakiuchi, M. Yamauchi, N. Chatani, S. Murai, Chem. Lett. (1996) 111. (c) T. Fukuyama, N. Chatani, F. Kakiuchi, S. Murai, J. Org. Chem. 62 (1997) 5647.

[3] (a) S. Otsuka, T. Yoshida, A. Nakamura, Inorg. Chem. 6 (1967) 20. (b) A. De Cian, R. Weiss, Acta Crystallogr. B28 (1972) 3264. (c) A.M. Brodie, B.F.G. Johnson, P.L. Josty, J. Lewis, J. Chem. Soc. Dalton Trans. (1972) 2031. (d) M.F. Semmelhack, C.H. Cheng, J. Organomet. Chem. 393 (1990) 237. (e) H.-J. Knölker, P. Gonser, Synlett (1992) 517. (f) H.-J. Knölker, P. Gonser, P.G. Jones, Synlett (1994) 405. (g) H.-J. Knölker, G. Baum, P. Gonser, Tetrahedron Lett. 36 (1995) 8191. (h) H.-J. Knölker, H. Goesmann, P. Gonser, Tetrahedron Lett. 37 (1996) 6543. (i) L.A.P. Kane-Maguire, S.G. Pyne, A.F.H. Siu, B.W. Skelton, J. Aust. Chem. 49 (1996) 673. (j) H.-J. Knölker, G. Baum, N. Foitzik, H. Goesmann, P. Gonser, P.G. Jones, H. Röttele, Eur. J. Inorg. Chem. (1998) 993.

[4] (a) J. Yin, J. Chen, W. Xu, Z. Zhang, Y. Tang, Organometallics 7 (1988) 21. (b) T.N. Danks, S.E. Thomas, J. Chem. Soc. Perkin Trans. (1990) 761.

[5] (a) A.J. Pearson, Acc. Chem. Res. 13 (1980) 463. (b) R. Grée, Synthesis (1989) 341. (c) H.-J. Knölker, Synlett (1992) 371. (d) W.R. Roush, C.K. Wada, J. Am. Chem. Soc. 116 (1994) 2151.

[6] (a) M. van Wijnkoop, R. Siebenlist, J.M. Ernsting, P.P.M. de Lange, H.-W. Frühauf, E. Horn, A.L. Spek, J. Organomet. Chem. 482 (1994) 99. (b) N. Feiken, H.-W. Frühauf, K. Vrieze, J. Fraanje, K. Goubitz, Organometallics 13 (1994) 2825. (c) N. Feiken, H.-W. Frühauf, K. Vrieze, N. Veldman, A.L. Spek, J. Organomet. Chem. 511 (1996) 281 and literature cited therein.

[7] W. Imhof, A. Göbel, D. Braga, P. De Leonardis, E. Tedesco, Organometallics 18 (1999) 736.

[8] (a) W. Imhof, J. Organomet. Chem. 533 (1997) 31. (b) W. Imhof, J. Organomet. Chem. 541 (1997) 109. (c) M.M. Bagga, W.T. Flannigan, G.R. Knox, P.L. Pauson, F.J. Preston, R.I. Reed, J. Chem. Soc. (C) (1968) 36. (d) W. Imhof, Poster Presentation at the XIIth FECHEM Conference on Organometallic Chemistry, Prague, Hungary, 1997. (e) W. Imhof, D. Berger, Poster Presentation at the XVIIIth ICOMC, Munich, Germany, 1998. (f) P.E. Baike, O.S. Mills, Chem. Commun. (1996) 707. (g) H.J. Knölker, E. Baum, P. Gouser, G. Rohde, H. Röttele, Organometallics 18 (1998) 3917.

[9] (a) N.S. Nametkin, V.D. Tyurin, V.V. Trusov, A.S. Batsanov, Y.T. Struchkov, J. Organomet. Chem. 219 (1981) C26. (b) N.S. Nametkin, V.D. Tyurin, V.V. Trusov, A.I. Nekhaev, G.G. Alexandrov, N.A. Parpiev, M.T. Tashev, H.B. Doustov, J. Organomet. Chem. 276 (1984) 199. (c) N.S. Nametkin, V.D. Tyurin, V.V. Trusov, A.I. Nekhaev, A.S. Batsanov, Y.T. Struchkov, J. Organomet. Chem. 302 (1986) 243.

[10] G.G. Aleksandrov, Y.P. Sobolev, A.I. Nekaev, M.T. Tashev, K.B. Dustov, N.S. Nametkin, V.D. Tyurin, Izv. Akad. Nauk. SSSR, Ser. Khim. (1986) 2534.

[11] (a) C.J. Elsevier, W.P. Mul, K. Vrieze, Inorg. Chim. Acta 198 (1992) 689 and literature cited therein. (b) W. Imhof, J. Chem. Soc. Dalton Trans. (1996) 1429. (c) W.P. Mul, C.J. Elsevier,

L.H. Polm, K. Vrieze, M.C. Zoutberg, D. Heijdenrijk, C.H. Stam, Organometallics 10 (1991) 2247.

[12] T. Carofiglio, S. Stella, C. Floriani, A. Chiesi-Villa, C. Guastini, J. Chem. Soc. Dalton Trans. (1989) 1957.

[13] (a) C.A. Mirkin, K.-L. Lu, G.L. Geoffroy, A.L. Rheingold, D.L. Staley, J. Am. Chem. Soc. 111 (1989) 7279. (b) C.A. Mirkin, K.-L. Lu, G.L. Geoffroy, A.L. Rheingold, J. Am. Chem. Soc. 112 (1990) 461. (c) J.-S. Song, S.-H. Han, S.T. Nguyen, G.L. Geoffroy, A.L. Rheingold, Organometallics 9 (1990) 2386. (d) C.A. Mirkin, K.-L. Lu, T.E. Snead, B.A. Young, G.L. Geoffroy, A.L. Rheingold, B.S. Haggerty, J. Am. Chem. Soc. 113 (1991) 3800. (e) T.E. Snead, C.A. Mirkin, K.-L. Lu, S.-B.T. Nguyen, W.-C. Feng, H.L. Beckmann, G.L. Geoffroy, Organometallics 11 (1992) 2613.

[14] (a) R.L. Bennett, M.I. Bruce, B.L. Goodall, M.Z. Iqbal, F.G.A. Stone, J. Chem. Soc. Dalton Trans. (1972) 1787. (b) A. Basu, S. Bhaduri, K. Sharma, P.G. Jones, J. Chem. Soc. Chem. Commun. (1987) 1126.

[15] (a) G. Hogarth, J. Organomet. Chem. 407 (1991) 91. (b) J.R. Shapley, S.I. Richter, M. Tachikawa, J.B. Keister, J. Organomet. Chem. 94 (1975) C43. (c) K.-W. Lee, T.L. Brown, Organometallics 4 (1985) 1030. (d) Z. Xue, W.J. Sieber, C.B. Knobler, H.B. Kaesz, J. Am. Chem. Soc. 112 (1990) 1825. (e) A.F. Dyke, S.A.R. Knox, M.J. Morris, P.J. Naish, J. Chem. Soc. Dalton Trans. (1983) 1417.

[16] G. Brauer, Handbuch der Präp. Anorg. Chemie, Part C, No. 1, 8th ed., VCH, Weinhem, 1968, p. 19.

[17] (a) G. Sheldrick, SHELXS-86, Universität Göttingen 1986. (b) G. Sheldrick, SHELXL-93, Universität Göttingen 1993.

[18] L. Zsolnai, G. Huttner, XPMA, Universität Heidelberg, Germany, 1996.

[19] Siemens Analytical X-ray Instruments Inc., XP-Interactive Molecular Graphics, Version 4.2, 1990.

[20] (a) **1**: P.W. Westermann, R.E. Botto, J.B. Roberts, J. Org. Chem. 43 (1978) 2590. (b) **2**, **3**: A.F.M. Iqbal, J. Org. Chem. 37 (1972) 2791. (c) **4**: A.R. Bassindale, A.G. Brook, P.F. Jones, J.A.G. Stewart, J. Organomet. Chem. 152 (1978) C25.